NASA Contractor Report 185261

Flat Tensile Specimen Design
for Advanced Composites

Dennis W. Worthem

Sverdrup Technology, Inc.
Lewis Research Center Group
Brook Park, Ohio

November 1990

Prepared for
Lewis Research Center
Under Contract NAS3-25266

NASA

National Aeronautics and
Space Administration

NASA
National Aeronautics and
Space Administration

Report Documentation Page

1. Report No. NASA CR-185261	2. Government Accession No.	3. Recipient's Catalog No.

4. Title and Subtitle	
Flat Tensile Specimen Design for Advanced Composites	5. Report Date November 1990
	6. Performing Organization Code

7. Author(s)	
Dennis W. Worthem	8. Performing Organization Report No. None (E-5602)
	10. Work Unit No. 510-01-01

9. Performing Organization Name and Address	
Sverdrup Technology, Inc. Lewis Research Group 2001 Aerospace Parkway Brook Park, Ohio 44142	11. Contract or Grant No. NAS3-25266
	13. Type of Report and Period Covered Contractor Report Final

12. Sponsoring Agency Name and Address	
National Aeronautics and Space Administration Lewis Research Center Cleveland, Ohio 44135-3191	14. Sponsoring Agency Code

15. Supplementary Notes

Project Manager, Paul Chorna, Structures Division, NASA Lewis Research Center.

16. Abstract

Finite-element analyses of flat, reduced-gage-section tensile specimens with various transition region contours were performed. Within dimensional constraints, such as maximum length (15.2 cm), tab region width (1.27 cm), gage width (1.106 cm), gage length (1.52 cm), and minimum tab length (3.18 cm), a transition contour radius of 41.9 cm produced the lowest stress values in the specimen transition region. The stresses in the transition region were not sensitive to specimen material properties. The stresses in the tab region were sensitive to specimen composite and/or tab material properties. An evaluation of stresses with different specimen composite and tab material combinations must account for material nonlinearity of both the tab and the specimen composite. Material nonlinearity can either relieve stresses in the composite under the tab or elevate them to cause failure under the tab.

ORIGINAL CONTAINS
COLOR ILLUSTRATIONS

17. Key Words (Suggested by Author(s))	18. Distribution Statement
Tensile specimen; Transition; Gage section; Tab; Finite element analysis; Composite; Mechanical testing	Unclassified – Unlimited Subject Category 24

19. Security Classif. (of this report) Unclassified	20. Security Classif. (of this page) Unclassified	21. No. of pages 17	22. Price* A03

NASA FORM 1626 OCT 86   *For sale by the National Technical Information Service, Springfield, Virginia 22161

FLAT TENSILE SPECIMEN DESIGN FOR ADVANCED COMPOSITES

Dennis W. Worthem
Sverdrup Technology, Inc.
Lewis Research Center Group
Brook Park, Ohio 44142

SUMMARY

Flat, reduced-gage-section tensile specimens are used for the mechanical testing of advanced composites. Current configurations frequently fail in the transition region between the gage section and the tab region, producing low values of ultimate tensile strength and shorter fatigue lives. Failure in the tab region is associated with the use of certain tab materials. The goal of this study was to determine and evaluate a specimen design that will produce more consistent failures in the straight-sided gage section. Also, tab material and specimen composite combinations were evaluated for their ability to avoid failure in the tab region.

Finite-element analyses of flat, reduced-gage-section tensile specimens with various transition region contours were performed. Within dimensional constraints, such as maximum length (15.2 cm), tab region width (1.27 cm), gage width (1.106 cm), gage length (1.52 cm), and minimum tab length (3.18 cm), a transition contour radius of 41.9 cm produced the lowest stress values in the specimen transition region. The stresses in the transition region were not sensitive to specimen material properties.

The stresses in the tab region were sensitive to specimen composite and/or tab material properties. An evaluation of stresses with different specimen composite and tab material combinations must account for material nonlinearity of both the tab and the specimen composite. Material nonlinearity can either relieve stresses in the composite under the tab or elevate them to cause failure under the tab.

INTRODUCTION

New classes of composite materials have been proposed for applications involving severe thermomechanical loading. Extensive testing is required to generate reliable data on composite mechanical behavior for design, analysis, and processing studies. Critical to this task are specimen designs that can provide reliable and reproducible data.

Such types of tests as monotonic tension, tensile static, and cyclic loads at high temperatures require specimens with a reduced gage section. This type of gage section, which produces a homogeneously stressed volume of material at a uniform temperature, provides unambiguous results by forcing the failures to occur in this uniformly heated and stressed region.

Concerns with the use of the reduced-gage-section specimens focus on failures occurring in the transition region, an area between the tab region and the gage section, due to stress concentrations there and on failures occurring in the tab region under or near the tabs. Failures in these regions usually result in lower values of ultimate strength and time or cycles to failure. Therefore, much effort has been directed toward improving tensile testing procedures to minimize localized damage and stress concentration. This paper addresses these issues and proposes a tensile specimen design that reduces the chance of undesired failures locations.

BACKGROUND

Most fiber-reinforced, high-temperature composites are currently available only in relatively thin-plate form. Therefore, most tensile testing to date has been performed with specimen designs similar to that shown in figure 1. The middle of the specimen has a straight-sided gage section that is 3.81 cm long and 0.795 cm wide. Each end of the specimen has a straight-sided region that is 3.99 cm long and 1.27 cm wide, where the tabs are bonded. The transition between the gage section and the tab region is accomplished by a radius (6.35 cm) contour. The transition region begins at the end of the straight-sided gage section and ends at the beginning of the tab region.

In the tab region, tabs are bonded to each face of the
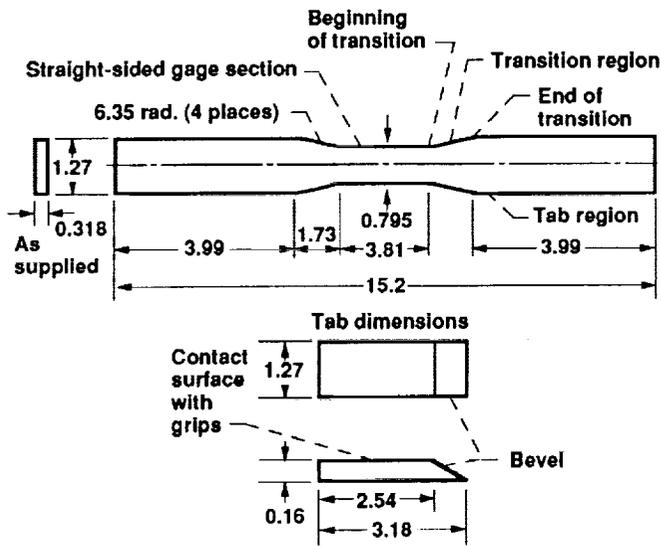
Figure 1.—Dimensions and terminology of a reduced-gage-section tensile specimen design used at NASA Lewis.

specimen with an adhesive. The tabs provide sufficient specimen thickness to fit into the grips. Tabs, which are made of relatively compliant and/or ductile materials, are also used to ensure uniform contact onto the specimens since the as-received material may have thickness variations.

Stress Distribution in the Specimen

In a reduced-gage-section specimen such as the one shown in figure 1, localized stress concentrations occurring in the transition region are caused by the reducing contour there (refs. 1 to 4). This is illustrated in figure 2. The maximum value of τ_{xy} occurs along the edge of the specimen near the end of the transition contour where the slope approaches a maximum. However, because the edge of the tab region is horizontal and traction free (τ_{xy} is zero), the maximum value of τ_{xy} occurs some distance away from the end of the transition. The maximum value of σ_x
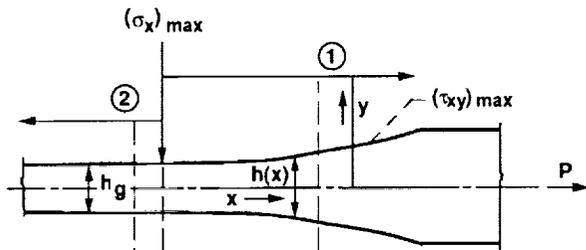
Figure 2.—Schematic illustrating the locations of maximum σ_x and τ_{xy} in the transition region of a reduced-gage-section specimen. Region 1 is the transition region of width h(x), and region 2 is the straight-sided gage section of width h_g (refs. 1 to 3).

occurs at the beginning of the transition region where the curvature of the edge starts abruptly.

One aspect of designing an improved tensile specimen involves producing a transition with minimal slope and with a small curvature or a curvature that gradually approaches zero near the beginning of the transition region. As a result, the maximum values of σ_x and τ_{xy} will be minimized. This can be demonstrated conveniently only by a finite-element analysis since it is difficult to find an Airy stress function that satisfies both the governing equations of elasticity and the boundary conditions of the problem. For unidirectional composites a maximum value of τ_{xy} that is less than 1/20 of the nominal σ_x in the gage section is used to prevent longitudinal splitting (refs. 1 to 3).

In the tab region, the load is transferred from the grips to the tab by stick-friction shear loads. Pressure is applied to the tabs to keep the specimen from slipping in the grips. The combination of shear and compression produces a three-dimensional state of stress that can only be conveniently described with finite-element analysis. One of the goals in tab design is to prevent failure in the tab region. The ASTM Test Method for Tensile Properties of Fiber-Resin Composites (D3039-76) specifies that for a valid test in a straight-sided specimen the failure should be at least one gage section width away from the tab end.

Failure Locations in Tensile Specimens

To date, testing of advanced composites has given varying results with regard to failure location, depending on the type of composite. Table I shows the percentage of the occurrence of failure locations during monotonic tension and tensile cyclic load testing at NASA Lewis of various composites (ref. 5). Also shown for comparison are the failure locations in straight-sided specimens with tabs. The straight-sided specimen has been a standard (ASTM D3039-76) for testing polymers unidirectionally reinforced with high modulus fibers and polymeric matrix composite tabs.

Most of the results in table I are for composites that are unidirectionally reinforced. Although applications will probably involve complex laminates, weaves, and braids, the performance of unidirectional reinforced plates is of interest in micromechanical modeling and processing studies. Most of the problems encountered are with unidirectionally reinforced plates because of the anisotropic behavior of the plates. Additionally, the strength of the composite can vary because of the directionality of the composite and any machining damage in the test specimens. However, cross and angle-ply laminates have also exhibited some problems (ref. 5).

Table I reveals the tendency for reduced-gage-section specimens to fail in the transition region for most of the

composite systems tested. The number of failures in the transition region was greater in cyclic load tests than in monotonic tension tests. Transition region failures in metal and intermetallic matrix composites were transverse cracks near the beginning of the transition region. This tendency has been attributed to one or more of the following: machining damage (broken fibers), the local axial stress concentrations, and any bending or twist in the specimens due to small misalignments in the load frame (ref. 5).

Failure in brittle matrix composites with glass or glass-ceramic matrices initiated near the end of the transition region. The failure was usually initiated by longitudinal splitting from the edge of the specimen in the transition. The splitting propagated into the tab region, and subsequently, low-angle cracks propagated and coalesced in the transition region of the specimen. This longitudinal splitting has been attributed to the brittle interface material (e.g., carbon) and matrices in fiber-reinforced glass-ceramics (refs. 5 and 6). The interfaces and matrices crack as a result of the longitudinal shear stress in the transition. The maximum value of this stress occurs where the slope of the contour approaches its maximum value (see the earlier discussion). Machining damage such as fiber fracture and pullout and matrix cracking may also contribute to this weakness (ref. 5).

Composites with ductile matrices and fibers which are well bonded to each other (such as the tungsten fiber/copper matrix system) consistently fail in the gage section (ref. 5). Inelastic deformation relieves the stress concentrations in the transition, and the good bonding between the fiber and matrix minimizes machining damage.

Straight-sided specimens of metal and intermetallic matrix composites with stainless steel tabs had a strong tendency to fail in the tab region. The intermetallic matrix composites failed at the end of the tab, and the metal matrix composites failed approximately 1/4 to 1/2 in. inside the tabs. The intermetallic matrix composite's behavior is explained by its extreme brittleness at room temperature compared with its high temperature behavior (ref. 5). The failure occurs at the stress concentrations in the tab region where the temperature is lower than the center of the specimen. The fracture location behavior of metal matrix composites has not been explained.

The glass and glass-ceramic matrix composite specimens with epoxy-fiberglass tabs failed in the gage section.

These failure locations for fiber-reinforced materials are of concern because the quantitative results may be too design specific and may not reflect behavior in the uniform stress and temperature regions. Various laboratories have proposed improved tensile specimen designs to replace the tabbed, straight-sided specimen for polymeric matrix composites. The need was for an acceptable reduced-gage-section specimen for harsh environment testing. Oplinger et al. (refs. 1 to 3) reviewed the various

proposed designs and presented stress analysis results for each.

Proposed Tensile Specimen Designs for Advanced Composites

The five specimen designs shown in figures 3 have been proposed in recent years for high-temperature testing of composites.

The straight-sided specimen (fig. 3(a)), with proper tabbing and gripping methods, has successfully provided many gage section failures at room temperature. However, at high temperatures potential problems, such as environmental deterioration of the tabs, statistical variation of preexisting flaw sizes, and the strengthening of the composite with temperature, increases the likelihood of failure outside the uniformly heated region gage section.

Figure 3(b) shows a specimen that has a transition region consisting of a radius and one of its tangents. This design, called the tangent-radius design (private communication with R. Tucker, Pratt & Whitney Aircraft Co.), produces a linearly increasing gage width with a small slope from near the beginning of the transition region. The maximum longitudinal shear stress is lower than that of the specimen shown in figure 1, and, consequently, the chance of longitudinal splitting is decreased. However, the tensile stress (σ_x) concentration at the beginning of the transition region is not reduced, and therefore the probability of failure at that location would not be reduced. For brittle matrix composites, the shear stress in the transition region may still not be low enough to prevent longitudinal splitting.

The "bow tie" and the double-reduced specimens (the former is similar to the tangent-radius specimen) shown in figures 3(c) and (d) also have lower shear stress concentrations but do not have lower tensile stress (σ_x) concentrations at the beginning of the transition region (refs. 1 to 4). Testing of these specimen designs produced failures in the transition region. A further consideration is that designs, such as the double reduced specimen, waste material and frequently rely on wedge loading, which can produce load train misalignments.

Another proposed design, called the streamline design (refs. 1 to 3), is based on an analogy from fluid mechanics. Its edges in the transition region have very small slopes and curvatures (fig. 3(e)). Therefore, the maximum values of σ_x and τ_{xy} are minimized. Finite-element analyses revealed that the normal and shear stress concentrations in the transition region were the lowest of the designs analyzed by Oplinger et al. (refs. 1 to 3). Test results for unidirectionally reinforced polymeric matrix composite samples with this design produced the highest average tensile strengths with the lowest coefficients of variation. Also, the streamline design produced longer

3
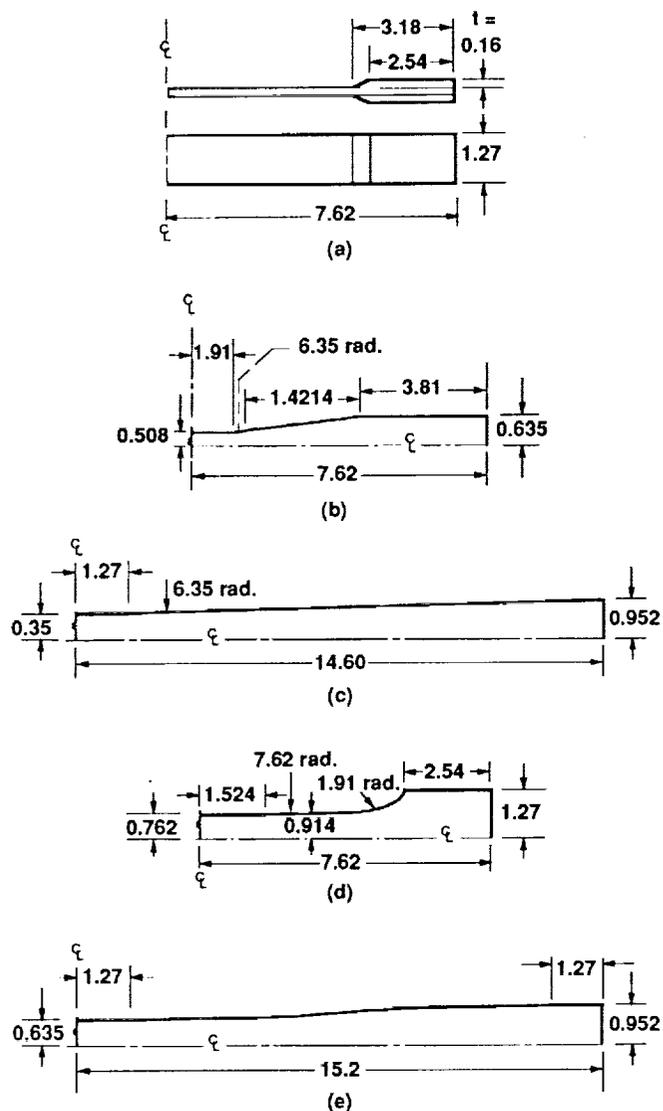
Figure 3.—Dimensions of proposed designs to replace the specimen shown in figure 1: (a) straight-sided, (b) tangent-radius, (c) bowtie, (d) double-reduced, and (e) streamline. One-half of a specimen is shown for (a) and one-quarter for (b) to (e). All the specimens would be machined from thin plates. Tab dimensions are shown in (a) that would be used for all the specimens analyzed in this report.

fatigue lives with less scatter than did the small-radius (7.62 cm rad.) design.

Concerns with the streamline specimen focus on the long gradual contour. The first is whether such a contour can be machined economically because of the small curvatures involved (fifth decimal place accuracy is required near the beginning of the transition). Experience by Oplinger et al., has shown, however, that the specimens can be machined economically within the dimensional tolerances possible with proper equipment. The second is that a long specimen is needed (25.4 to 33.0 cm long) in

order to produce a contour that is sufficiently gradual to limit the stress concentrations. Most new high-temperature composites are available only in smaller plates (15.2 cm by 15.2 cm or 20.3 cm by 20.3 cm). Therefore, it is desirable to limit the length to 15.2 to 20.3 cm but still use the streamline contour or some similar shape.

Specimen Designs Analyzed With Finite Elements

The goal of this research was to design a specimen using one of the streamline contours developed by Oplinger et al., and to scale and limit the contour length to produce a total specimen length of 15.2 or 20.3 cm with other dimensions as shown in figure 4. This limitation is reasonable since the local normal and shear stresses at the contour boundaries are determined by the local curvature and slope, as discussed before. Additionally, a large radius transition (ref. 4) whose total length is equal to that of the streamline's design was investigated. The large radius design is appealing because of the simplicity of the machining instructions for its fabrication; whereas the streamline design requires a detailed set of coordinate points for the contour.

Figure 5 illustrates the transition contours for a 6.35-cm radius, the streamline design, a 36.8 cm radius, and a 41.9 cm radius. For the 41.9-cm-radius design, tab region length was reduced to 3.60 cm (from 3.81). The large curvature of the 6.35-cm radius compared with the other contours is obvious, and higher tensile and shear stresses were expected in the transition region for this design. Because the streamline and large radii contours near the beginning of the transition are nearly identical, all were expected to exhibit similar tensile stress concentrations. However, near the end of the transition, the large radius contours have a smaller slope than the streamline contour, and, therefore, a smaller shear stress was expected along the specimen edge. In light of this discussion the large radius design was expected to perform the best at minimizing both axial and shear stress concentrations. Finite-element analysis was used to verify this prediction.
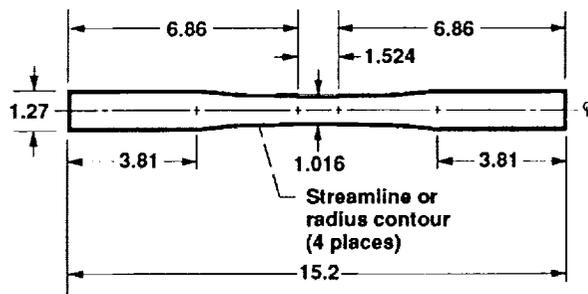
Figure 4.—Overall dimensions used for the analysis of the streamline and radius contour specimens. The tangent-radius specimen dimensions were those shown in figure 3(b).

4
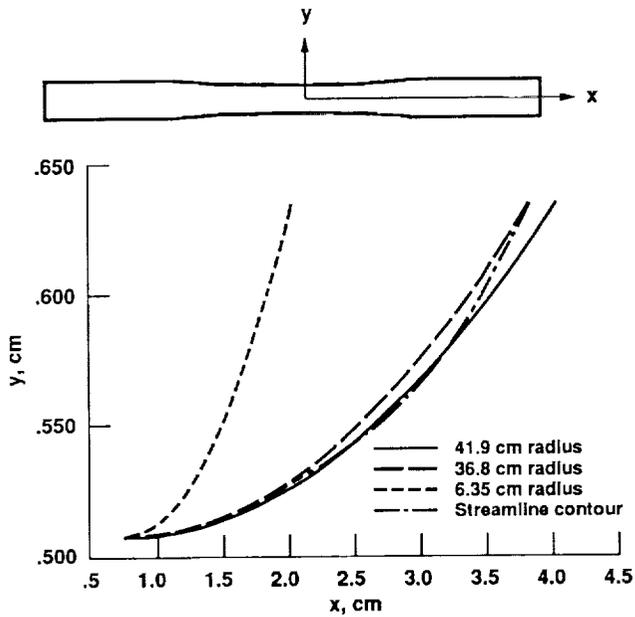
Figure 5.—Plot of the theoretical x-y coordinates of one edge of the transition region for specimens with four contours: 6.35 -cm radius, streamline, 36.8-cm radius, and 41.9-cm radius.

In this study specimens with radius, tangent-radius, and streamline contours in the transition regions were subjected to finite-element analysis, and the optimal design determined. Constitutive properties were used that are representative of the specimen composites and tab materials of interest.

ANALYSIS

The pre- and postprocessing for the finite-element analyses were performed using Patran (ref. 7). Figure 6 shows an example of a mesh. Eight-noded solid isoparametric elements were used. In figure 6(a) a total of 1176 elements and 1267 nodes were used. The number of elements varied slightly between specimen designs. In regions where stress concentrations were expected, such as near the specimen boundary in the transition and in the tab region near the end closest to the transition, the mesh was refined. The three-dimensional, linear elastic finite-element analyses were conducted using MARC (ref. 8). The specimen composites and tab materials were assumed to be homogeneous. Such assumptions greatly simplified and speeded the analyses because inelastic constitutive
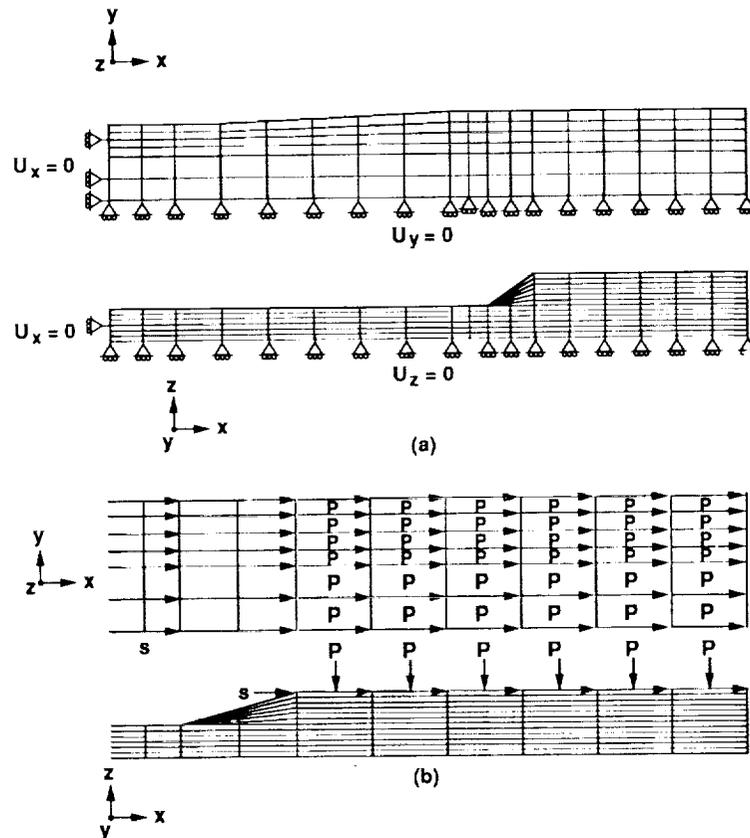
(a) Displacement boundary conditions.
(b) Load boundary conditions on the face of the tab. Shown are the pressure (p) and nodal shear (s) forces that would be applied by the grips.
Figure 6.—Finite-element mesh of one-quarter of a specimen.

models based on micromechanics of composites are still being developed. The analyses allowed a comparison on an unambiguous basis.

One-quarter of a specimen was analyzed with displacement boundary conditions imposed as shown in figure 6(a). The specimen composite was assumed to always be 0.318 cm thick. The displacement boundary conditions were imposed by setting to zero the normal displacements on the three planes of symmetry. The load was applied to the composite specimen through the tabs. The tab design selected (shown in fig. 1) was based on an analysis done by Cunningham et al. (ref. 9). The clamping load was simulated by a compressive load that was approximately 12 times the nominal axial load at failure in the gage section. The axial load was transmitted by nodal shear forces. Perfect contact was assumed between the tab and the specimen with no slip friction.

Tables II and III show the elastic properties used for the composites and tab materials. Additional analyses were performed on some of the specimens by accounting for any material nonlinearity in either the tab or the specimen composite. For materials that are ductile, such as metal tabs, the elastic-inelastic properties can be obtained from widely published data. A metal matrix in a composite may also deform plastically. Glass, glass-ceramic, and ceramic matrix composites reinforced by fibers deform nonlinearly because of matrix cracks which are bridged by fibers. Multiaxial constitutive laws for these composites are not yet available, so a von Mises yield criterion was assumed for all materials. Tables II and III list the nonlinear properties. Composite nonlinear properties were taken from uniaxial monotonic stress-strain tests performed at Lewis. The inelastic strain was obtained by subtracting the elastic strain (based on the initial axial Young's modulus) from the total strain.

The analysis was performed for four specimen designs of 15.2-cm-long material: a reduced gage section with a 6.35-cm radius, a tangent-radius with a 6.35-cm radius, streamline contour, and a reduced gage section with a 36.8-cm radius for the transitions. All designs have gage lengths and widths of 1.524 and 1.016 cm, respectively, and tab region lengths and widths of 1.27 and 3.81 cm, respectively. Figure 4 illustrates the basic specimen dimensions for all but the tangent-radius specimen, the dimensions for which are shown in figure 3(b). The 1.52-cm gage length permits the use of an extensometer with a 1.27-cm gage length. The 3.81-cm tab-region was shortened (to 3.60 cm) to accommodate a 41.9-cm radius transition region. Analyses showed that the region between the end of the transition and the beginning of the tab was long enough to prevent significant interaction between the two regions, thereby permitting the shorter (3.60 cm) tab length.

RESULTS

All values of the elastic moduli and of stress were normalized by the ultimate tensile strength of the composite occurring nominally in the gage section. In the transition region, the goal was to have the maximum value of σ_x as close to 1.00 as possible and the maximum value of τ_{xy} less than 0.05. In the tab region the goal was to have the maximum values of all the normal stress components less than 1.00 and the maximum values of all the shear stress components less than 0.05. In the tab material the goal was to have the maximum values of all the normal stress components less than the ultimate tensile strength of the tab material and the maximum value of the shear stresses less than about half the ultimate tensile strength of the tab material. It was assumed that the composite or tab could fail independently, in response to each component of stress. If more than one of the stress components was relatively high at one location, then an effective stress would be required to predict the likelihood of failure at that location (multiaxial continuum damage criterion).

Transition Region

Figures 7 and 8 show the results of a linear elastic analysis for the normal (σ_x) and in-plane shear (τ_{xy}) stress contours in the 6.35-cm-radius reduced-gage-section specimen. The specimen was made of a metal matrix composite (SiC[0°]/Ti-15-3-3-3) with stainless steel tabs. The maxima of these stress components were in the transition region. The maximum normal stress was 4 percent higher than the nominal gage-section normal stress and was located 0.20 cm from the beginning of the transition region. The shear stress reached a maximum of 0.106 at 0.84 cm from the beginning of the transition region. This value of 0.106 was more than twice the 0.05 maximum desired shear stress (refs. 1 to 4). In the tab region the normal and shear stresses in the composite were all less than about 0.870 and 0.030, respectively, and the maxima are located just outside the tab.

Table IV gives the numerical values of the maximum normal and shear stresses and their locations in the transition region for the specimen designs analyzed. For the metal matrix composites, the lowest values of these stresses were exhibited in the specimen with a 41.9-cm radius. For this design the maximum normal stress was 0.3 percent above the nominal gage-section stress and was located at the beginning of the transition region. The maximum shear stress was 0.0447, located 2.44 cm from the beginning of the transition region. In the tab region of the 41.9-cm radius specimen, the maximum normal and shear
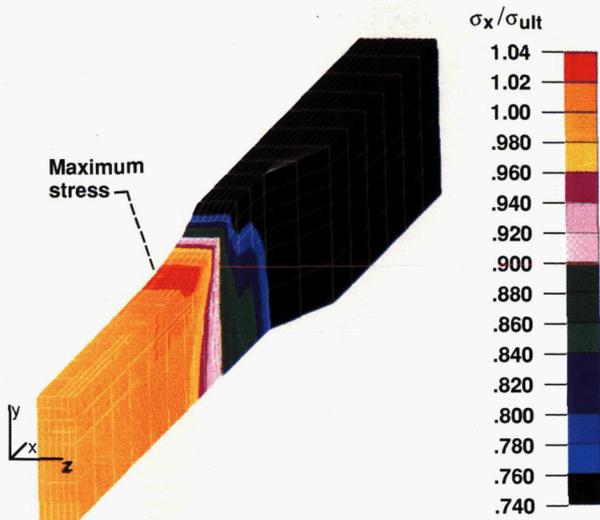
Figure 7.—Contours of σ_x/σ_{ult} in a specimen with a transition region contour of 6.35-cm radius. Gage section width, 1.016 cm; tab length, 3.81 cm; material, SiC[0°]/Ti-15-3-3-3 with stainless steel tabs; type of analysis, linear elastic. $\sigma_{x,max}/\sigma_{ult}$ = 1.04 located 0.20 cm from end of transition.
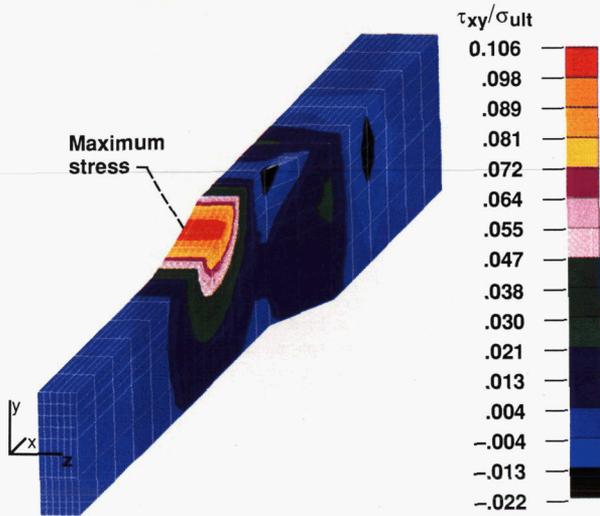
Figure 8.—Contours of τ_{xy}/σ_{ult} in a specimen with a transition region contour of 6.35-cm radius. Gage section width, 1.016 cm; tab length, 3.81 cm; material, SiC[0°]/Ti-15-3-3-3 with stainless steel tabs; type of analysis, linear elastic. $\tau_{xy,max}/\sigma_{ult}$ = 0.106 located 0.85 cm from end of transition.
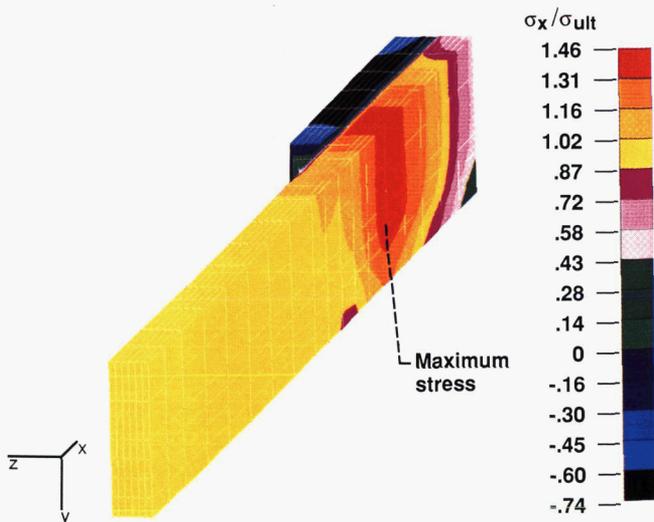
Figure 9.—Contours of σ_x/σ_{ult} in the tab region of a straight-sided specimen with a 3.18 cm long tab. Gage section width, 1.27 cm; specimen material, SiC[0°]/CAS with epoxy fiberglass tabs; type of analysis, linear elastic. $\sigma_{x,max}/\sigma_{ult}$ = 1.46 located 1.27 cm from end of tab, under the tab.

stresses in the composite were less than about 0.870 and 0.030, respectively, and were located just outside the tab. Comparison of these results with the other specimen transition contours showed that the contour design had little if any effect on the tab region stresses. This was due to the relatively large distance between the end of the transition and the beginning of the tab region.

Table IV gives one result for a nonlinear analysis for the same specimen design and tab-composite material combination as in figures 7 and 8. The maximum normal stress (σ_x) dropped from 1.04 to 1.02, and the maximum in-plane shear stress (τ_{xy}) did not change. Also, the location of these maximum stresses did not change from that in the elastic analysis.

Table IV indicates that the results were only slightly affected by change in specimen material. Although not shown, the other stress components (σ_y, σ_z, τ_{xz}, and τ_{yz}) were approximately zero.

Tab Region

In the elastic analyses discussed above, the normal (σ_x) and inplane shear (τ_{xy}) stresses in the tab region were not excessive (less than 1.00 and 0.05, respectively) for the metal matrix composite with stainless steel tabs. The other stress components (σ_y, σ_z, τ_{xz}, and τ_{yz}) were approximately zero. The fact that all the stresses were acceptable in the tab region is a result of a relatively close match in all the elastic properties of the specimen composite and the tab material (see tables II and III).

In none of the analyses done in this paper were the stresses in the tab material high enough to predict failure in the tab material before the composite. This is in agreement with experiment (ref. 5). For the case shown in figure 7, σ_x, σ_y, and σ_z all ranged from less than 1.00 to compression. Of the shear stresses τ_{xz} was the greatest, and this value was usually at most 0.40 near the tip of the bevel, which indicates that yielding of the tab may occur in the bevel region. In tests of a metal matrix composite with stainless-steel tabs, the straight bevel contour (see fig. 1) deformed into a concave contour, which is probably a result of this τ_{xz} (ref. 5).

The use of tab materials with elastic moduli much different (e.g., by a factor of two) from the specimen composite produced severe stress concentrations in the composite. This is illustrated in figure 9 which shows the contours of σ_x in the tab region (3.18 cm long tab) for a silicon carbide (SiC) fiber-reinforced glass ceramic with a fiberglass-reinforced epoxy in a specimen with a straight-sided specimen design (see tables I and II to compare the elastic properties of the specimen composite and tab materials.) A concentration of 46 percent existed in the composite under the tab. This result indicates that failure is expected in the tab region. However, experimental results

indicate that the majority of failures are outside the tab region (ref. 5).

In a straight-sided specimen the normal stress concentration can be reduced by increasing the length of the tab. This decreases both the clamping pressure (given the same clamping load) and the shear stress on the tab surface. In a straight-sided specimen of SiC-fiber-reinforced glass ceramic with a 5.08-cm-long fiberglass-reinforced epoxy tabs, the maximum σ_x was 1.22. This compared with a $\sigma_{x,max}$ of 1.46 for a specimen of the same design and materials but with a shorter tab (3.18 cm).

Figure 10 shows the result of an analysis for a straight-sided specimen that accounts for the nonlinearity in the stress-strain behavior of the glass-ceramic composite caused by matrix cracking in the specimen. The stresses in the specimen under the tab were all less than 1.00. There was a concentration of stress just outside the tab, where the maximum value of σ_x was 1.02. However, the volume of material at this stress was small so the majority of failures would be expected in the gage section (at least one specimen width from the tip of the tabs as per ASTM D3039), as confirmed by experiment (ref. 5). Posttest examination of tensile specimens showed periodic matrix cracking under the tab up to the area of highest stress indicated by the elastic analysis. Thus, nonlinearity due to matrix cracking in the composite probably aids in avoiding tab region failures by relieving the stresses in the composite. The maximum σ_x was 1.05 in a nonlinear analysis when a 3.18 cm tab was used, which indicated that longer tabs aid in reducing the chance of failure under or near the tabs.

Table V shows the location and value of σ_x in both straight-sided and reduced-gage-section specimens for the specimen composite and tab material combinations studied. The results of the glass-ceramic composites with polymeric composite tabs in a straight-sided specimen have already been discussed. In a reduced-gage-section specimen, the epoxy-fiberglass tab is suitable for the glass-ceramics. Copper (or aluminum) could have been selected as the tab material based on its elastic properties; however, when nonlinearity of the tab and specimen materials were accounted for, there was a maximum σ_x of 2.20 in, for example, a reduced-gage-section specimen. Therefore, failure in the composite under the tab is expected in reduced-gage-section specimens (with dimensions as in fig 4) with tabs of metals like copper (or aluminum).

For the SiC-reinforced titanium alloy with a 3.18-cm-long stainless-steel tabs, $\sigma_{x,max}$ increased from 1.04 to 1.36 in a straight-sided specimen from linear to nonlinear analyses, respectively. The location of this maximum stress changed from just outside the tab in a small volume of material to under the tab about 1.90 cm from the end of the specimen with a relatively large cross section at a high stress. Experimental results confirm that there is a tendency to fail at this location (ref. 5). For the longer tab
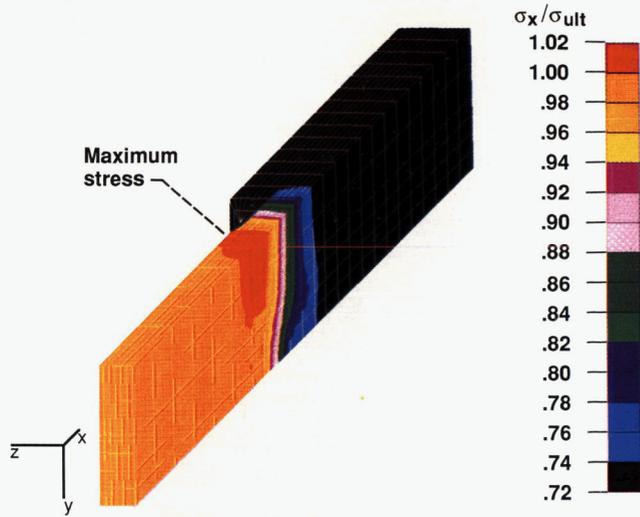
Figure 10.—Contours of σ_x/σ_{ult} in the tab region of a straight-sided specimen with a 5.08-cm long tab. Gage section width, 1.27 cm; specimen material, SiC[0°]/CAS with epoxy fiberglass tabs; type of analysis, linear elastic-nonlinear. $\sigma_{x,max}/\sigma_{ult}$ = 1.02 located 0.48 cm from end of tab, outside of the tab.
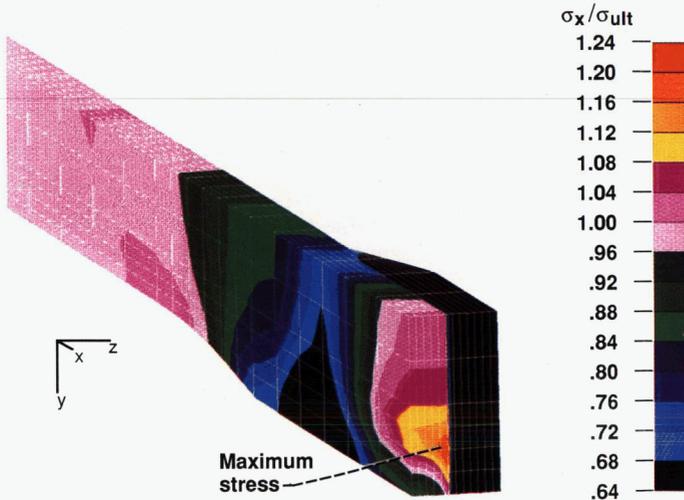
Figure 11.—Contours of σ_x/σ_{ult} in the tab region of a specimen with the dimensions of figure 3. The specimen and tab were sectioned 1.70 cm from the end of the specimen. Gage section width, 1.016 cm; tab length, 3.81 cm; specimen material, SiC[0°]/Ti-15-3-3-3 with stainless steel tabs; type of analysis, linear elastic-nonlinear. $\sigma_{x,max}/\sigma_{ult}$ = 1.21 located 1.70 cm from end of specimen, under the tab.
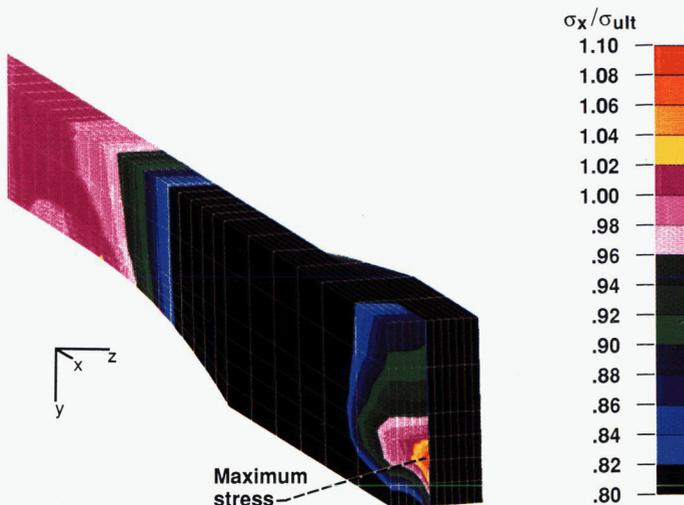
Figure 12.—Contours of σ_x/σ_{ult} in the tab region of a specimen with the dimensions of figure 1. The specimen and tab were sectioned 1.70 cm from the end of the specimen. Gage section width, 0.745 cm; tab length, 3.81 cm; specimen material, SiC[0°]/Ti-15-3-3-3 with stainless steel tabs; type of analysis, linear elastic-nonlinear. $\sigma_{x,max}/\sigma_{ult}$ = 1.09 located 1.70 cm from end of specimen, under the tab.

length of 5.08 cm, the maximum stress decreased from 1.36 to 1.05 in a nonlinear analysis. This again demonstrated that a longer tab reduces the chance of failure in the tab region. The maximum stress in the tab region decreased in a reduced-gage-section specimen. This value was 1.21 in a specimen with a 1.016-cm gage width (fig. 11) and 1.09 in one with a 0.795-cm gage width (fig. 12). For these last two cases, the decrease in $\sigma_{x,max}$ was accompanied by a decrease in the volume of material at a stress over 1.00. Thus, the 0.795-cm gage width specimen should rarely fail in the tab area, which agrees with experimental results. However, for the 1.016-cm gage width specimen (used in the proposed 41.9-cm-radius contour specimen) there may be some tendency to fail in the tab region. This suggests that a different tab material may be necessary.

Table V indicates that stainless steel is adequate for specimens with a reduced-gage-section geometry made of the SiC fiber/SiC matrix composite. Because this composite has a plain woven laminate fiber architecture, no analyses in this paper were performed for this composite using a straight-sided specimen design. The plain woven fiber architecture was expected to preclude many of the problems experienced when testing composites made of unidirectionally reinforced plies.

DISCUSSION

The finite-element analyses of this report suggests that more reliable test results may be obtained by employing an improved tensile specimen design. Increased reliability in this case would be evidenced by consistently producing gage-section failures. The reduced-gage-section specimen with a 41.9-cm radius provided the lowest values of τ_{xy} in the transition region and as low a value of σ_x at the end of the transition region as any other specimen. This specimen also produced a large separation between the locations of $\sigma_{x,max}$ and $\tau_{xy,max}$. This separation increased from 0.64 cm for a 6.35-cm radius to 2.44 cm for the 41.9-cm radius. A relatively large separation between these stresses reduces the combined state of stress which may determine the location of complete failure of the specimen. The specimen design is also simple with regard to machining instructions. With this geometry, a table of x-y coordinates is not required, in contrast to the streamline specimen.

However, the small curvature of the 41.9-cm-radius design also leads to the extension of the effective gage section into the transition region. This can be understood by considering that at 1.143 cm into the transition (i.e., 1.429 cm from the center of the gage section), the nominal value of σ_x has decreased by only 3 percent (see table VI). Specimens may fail at even this decreased stress because of statistical distributions of pre-existing flaw sizes in the

constituents. Using this value of 3 percent as an example, the effective gage section will be 3.81 cm rather than 1.525 cm. For high temperature tests, the preferred length of the uniformly heated zone would be 3.81 cm long also. For some materials that strengthen with temperature within a certain temperature range, the specimens may still fail outside the uniform temperature region since these regions will be weaker. For such materials and testing conditions, hot grips may alleviate the problem. The large radius design also does not directly deal with the problem of machining damage. As discussed in the introduction, failures in the transition may be caused by machining damage on the edges. This would be worse than on the straight-sided gage section or specimen because of the difficulty in translating the machining tool smoothly along a curved contour with a relatively large curvature. Perhaps the smaller curvature of a large radius contour will minimize the damage since this contour approaches that of a straight-sided specimen and, therefore, it would be easier to translate the machining tool along the contour.

The researcher should select a tab material based on the entire deformation response of both the tab and the specimen material, keeping in mind that the deformation behavior will also depend on fiber architecture. However, the tab material must have sufficient shear strength because of the large shear stresses (τ_{xz}) in the bevel region of the tab. This recommendation would be applicable to testing at loads above any proportional limit. Ideally, the tab material would be the same as the specimen composite. However, other considerations such as machinability and the directional strength characteristics of the composite may preclude the use of the same material for tabs. Also, a gripping method should be used that minimizes friction and clamping pressure. Friction can be minimized by using special surfaces on the collets or by surface preparation of the tab. The clamping pressure can be decreased by increasing both the friction and the tab length. Where polymeric composite tabs produce optimal results, substitutes must be sought for high-temperature testing. Perhaps a composite with a higher temperature matrix resin can be used. For complex fiber architectures and when subcritical loads are employed such as in creep and fatigue testing, tabs may not be necessary (if the gripping arrangement will accommodate the specimen thickness).

CONCLUSIONS

Finite-element analyses were performed to determine an optimal tensile specimen design for the new high-temperature composites. The objective was to minimize the stresses that would cause failure in the transition between the gage section and the tab regions. Additionally, the analyses included the study of several tab material and specimen composite combinations. The effect of tab

material and specimen composite nonlinearity was also analyzed. The following points were concluded:

1. Improved test results may be possible with contours other than a small radius (≤ 7.62 cm) transition regions. A large radius (41.91 cm) proved to have the lowest values of maximum normal stress (σ_x) and in-plane shear stress (τ_{xy}) and the largest separation between their locations.

2. The finite-element results for the transition region and for the straight-sided gage section were relatively insensitive to the specimen composite, indicating that the previous conclusion is applicable to most composites.

3. Use of the 41.91-cm-radius specimen design may require a uniform heat zone beyond the straight-sided gage section. This will ensure failure in the uniformly heated zone by accounting for statistical variations of composite strength and for composite strength differences influenced by temperature.

4. Tab materials should be selected by considering the entire deformation behavior, including any nonlinearity of the tab material and specimen composite as well as the machinability or the directional strength characteristics of the proposed tab material.

5. The tab should be as long as possible to reduce the clamping pressure and shear stress applied by the grips.

REFERENCES

1. Oplinger, D.W.; et al.: Comparison of Tension Specimen Designs for Static and Fatigue Testing of Composite Materials. Presented at the Second U.S.-Japan Symposium on Composite Materials, NASA Langley Research Center, Hampton, VA, June 1983.

2. Oplinger, D.W.; Gandhi, K.R.; and Parker, B.S.: Studies of Tension Test Specimens for Composite Materials. AMMRC TR-82-27, Apr. 1982. (Available from NTIS, AD-A120257.)

3. Oplinger, D.W.; et al.: On the Streamline Specimen for Tension Testing of Composite Materials. Recent Advances in Composites in the United States and Japan, J.R. Vincent and M. Taya, eds., ASTM STP-864, 1985, pp. 532-555.

4. Phillips, D.C.; and Davidge, R.W.: Test Techniques for the Mechanical Properties of Ceramic Matrix Fibre Composites. Br. Ceram. Trans. J., vol. 85, no. 4, July-Aug., 1986, pp. 123-130.

5. Bartolotta, P.A.; and Ellis, J.R.: Elevated Temperature Testing of Advanced Composites. Presented at the ASTM Fall Meeting, Nov. 1989.

6. Hartman, G.A.; Zawada, L.P.; and Russ, S.M.: Techniques for Elevated Temperature Testing of Advanced Ceramic Composite Materials, in Fifth Annual Hostile Environments and High Temperature Measurements Conference Proceedings, Society for Experimental Mechanics, Inc., 1988, pp. 31-38.

7. PDA/PATRAN II, User's Guide, PDA Engineering, Santa Ana, CA, 1989.

8. MARC General Purpose Finite Element Program, Marc Analysis Research Corp., Palo Alto, CA, 1989.

9. Cunningham, M.E.; Schoultz, S.V.; and Toth, Jr., J.M.: Effect of End-Tab Design on Tension Specimen Stress Concentrations in Recent Advances in Composites in the United States and Japan, ASTM STP-864, Philadelphia, 1985, pp. 253-262.

10. Gomina, M; Chermant, J.L.; and Osterstock, F.: Crack Propagation in C-SiC. Creep and Fracture of Engineering Materials and Structures, B. Wilshire and D.R.J. Owen, eds., Pinebridge Press, 1984, pp. 541-550.

TABLE I. - FAILURE LOCATIONS IN FLAT TENSILE SPECIMENS

(a) Reduced gage section specimens

Composite material type (a)	Composite material	Type of test	Failure location, percent	
			Gage section	Transition
MMC B/D	SiC/Ti-15V-3Cr-3Al-3Sn	Tension	80	20
IMC B/B	SiC/Ti-24Al-11Nb	!	80	20
MMC D/D	W/Cu		100	---
MMC D/D	W/Kanthal		80	20
GMC B/B	SiC/AS Glass		---	100
GCMC B/B	SiC/CAS Glass-Ceramic	!	---	100
MMC B/D	SiC/Ti-15V-3Cr-3Al-3Sn	Fatigue	25	75
IMC B/B	SiC/Ti-24Al-11Nb	Fatigue	70	30
MMC D/D	W/Cu	Fatigue	100	---

(b) Straight-sided specimens

Composite material type (b)	Composite material	Type of test	Failure location, percent	
			Gage section	Tab region
IMC B/B	SiC/Ti-24Al-11Nb[h]	Tension	0	100
MMC B/D	SiC/Ti-15V-3Cr-3Al-3Sn[h]	!	50	50
GMC B/B	SiC/AS glass[c]		100	---
GCMC B/B	SiC/CAS glass-ceramic[c]	!	100	---
MMC B/D	SiC/Ti-15V-3Cr-3Al-3Sn[h]	Fatigue	100	---

[a]MMC - metal matrix composite
IMC - intermetallic matrix composite
GMC - glass matrix composite
GCMC - glass-ceramic matrix composite
B - brittle fiber or matrix
D - ductile fiber or matrix.
[h]Stainless steel tab.
[c]Fiberglass-reinforced epoxy tab.

12

TABLE II. - SPECIMEN COMPOSITE MATERIAL PROPERTIES

Property	SiC/Ti-15-3-3	SiC/CAS	SiC/SiC
	Fiber architecture		
(a)	Undirectional		Plain woven laminates[b]
E_{11}	[c]184.1 GPa	[d]124.1 GPa	[e]227.5 GPa
E_{22}	[c]129.6 GPa	[d]117.2 GPa	[e]227.5 GPa
E_{33}	~E_{22}	~E_{22}	[g]56.9 GPa
v_{12}	[c]0.28	[d]0.25	[e]0.15
v_{13}	[f]0.32	~v_{12}	[e]0
v_{23}	~v_{13}	~v_{12}	[e]0
G_{12}	[h]61.2 GPa	[h]48.3 GPa	[h]98.9 GPa
G_{13}	~G_{12}	~G_{12}	~G_{12}
G_{23}	~G_{12}	~G_{12}	~G_{12}
σ_{ult}	[c]1379 MPa	[d]444.7 MPa	[e]200 MPa
[i]σ_{pl}	[c]1103 MPa	[d]188.2 MPa	[e]69 MPa
$\sigma > \sigma_{pl}$ behavior	[c]Bilinear to a failure strain of 0.8 percent	[c]Used actual stress-strain curve to a failure strain of 1.01 percent	[e]Used actual stress-strain curve to a failure strain of 0.2 percent

[a]The subscript 1 indicates fiber direction; which is aligned with the x or axial direction; 2 indicates direction perpendicular to the fiber and in the plane of the specimen; 3 indicates the direction perpendicular to 1 and 2.

[b]All fibers are in the 1 and 2 directions.

[c]Measured at Lewis.

[d]Measured values obtained from Corning Glass.

[e]Measured values obtained from DuPont Co.

[f]Value for unreinforced matrix (isotropic).

[g]Estimated value based on similar carbon-fiber-reinforced SiC (ref.10).

[h]Estimated by $[(E_{11} + E_{22})/2]/[2(1 + v_{12})]$.

[i]Proportional limit.

13

TABLE III. - TAB MATERIAL PROPERTIES

Property (a)	Stainless steel[b]	Copper[c]	Fiberglass-reinforced epoxy[d]
E_{11}	193 GPa	110 GPa	18.6 GPa
E_{22}	$\approx E_{11}$	$\approx E_{11}$	15.2 GPa
E_{33}	$\approx E_{11}$	$\approx E_{11}$	$\sim E_{22}$
v_{12}	0.28	0.33	0.39
v_{13}	$\sim v_{12}$	$\sim v_{12}$	$\sim v_{12}$
v_{23}	$\sim v_{12}$	$\sim v_{12}$	$\sim v_{12}$
G_{12}	65.5 GPa	41.5 GPa	6.08 GPa
G_{13}	$\sim G_{12}$	$\sim G_{12}$	$\sim G_{12}$
G_{23}	$\sim G_{12}$	$\sim G_{12}$	$\sim G_{12}$
σ_{yield}	999.8 MPa	333 MPa	(e)
σ_{ult}	1068.7 MPa	551.6 MPa	434 MPa
n	0.0086	0.214	(e)
K	1090.8 MPa	551.6 MPa	(e)

[a]See footnote a, table II.
[b]Isotropic; 45 percent cold worked.
[c]OFHC; isotropic: hard drawn.
[d]NEMA grade GR-10.
[e]Assumed linear elastic to failure.

TABLE IV. - MAGNITUDE AND LOCATION OF $\sigma_{x,max}/\sigma_{ult}$ AND $\tau_{xy,max}/\sigma_{ult}$ FOR VARIOUS SPECIMEN

CONTOURS AND MATERIALS

Material	Specimen, cm	$\sigma_{x,max}/\sigma_{ult}$	Distance from beginning of transition region, cm	$\tau_{xy,max}/\sigma_{ult}$	Distance from beginning of transition region, cm	Distance between $\sigma_{x,max}$ and $\tau_{xy,max}$, cm
MMC (SiC|0°|/Ti alloy)	6.35-cm radius, 1.016-cm gage width	1.04	0.20	0.106	0.84	0.64
	6.35-cm radius, 1.016-cm gage width	1.02	0.20	0.106	0.84	0.64
	6.35-cm radius, 0.795-cm gage width	1.03	0.15	0.137	1.22	1.07
	Tangent-radius, 6.35-cm radius	1.04	0.18	0.0676	0.84	0.66
	Streamline	1.003	0	0.0563	2.46	2.46
	36.8-cm radius	1.003	0	0.0482	2.29	2.29
	41.9-cm radius	1.003	0	0.0447	2.44	2.44
GCMC (SiC|0°|/CAS)	Streamline	1.003	0	0.0568	2.46	2.46
CMC (SiC/SiC, plain woven laminates)	Streamline	1.002	0	0.0540	2.46	2.46

[a]Nonlinear analysis.

TABLE V. - MAGNITUDE AND LOCATION OF $\sigma_{x,max}/\sigma_{ult}$ IN THE TABBED REGION FOR

VARIOUS CONTOURS, MATERIALS, AND TAB MATERIALS

Specimen material (b)	Specimen geometry	Tab material, (b)	Tab length, cm	Type of analysis	$\sigma_{x,max}/\sigma_{ult}$	Location in specimen
GCMC (Si[0°]/CAS)	Straight-sided	PMC	3.18	Linear	1.46	Under tab
				Nonlinear	1.05	Just outside tab tip
			5.08	Linear	1.22	Under tab
				Nonlinear	1.02	Just outside tab tip
	Radius[a] with 1.016-cm gage width	PMC	3.18	Linear	2.31	Under tab
				Nonlinear	.94	Under tab
	Straight-sided	CU	3.18	Linear	1.04	Just outside tab tip
				Nonlinear	2.35	Under tab
			5.08	Linear	1.01	Just outside tab tip
				Nonlinear	1.02	Just outside tab tip
	Radius[a] with 1.016-cm gage width	CU	3.18	Linear	0.87	Just outside tab tip
				Nonlinear	2.20	Under tab
MMC (SiC[0°]/Ti alloy)	Straight-sided	SS	3.18	Linear	1.04	Just outside tab tip
				Nonlinear	1.36	Under tab
			5.08	Linear	1.04	Just outside tab tip
				Nonlinear	1.03	Just outside tab tip
	Radius[a] with 1.016-cm gage width	SS	3.18	Linear	0.87	Just outside tab tip
				Nonlinear	1.21	Under tab
	Radius[a] with 0.795-cm gage width	SS	3.18	Nonlinear	1.09	Under tab
CMC (SiC/SiC, plain woven laminates)	Radius[a] with 1.016-cm gage width	SS	3.18	Linear	0.94	Under tab
				Nonlinear	.95	Just outside tab tip

[a]Stresses in the tab region were not affected by the transition shape and size.

[b]MMC - SiC/Ti alloy (0°)　　　　　　　PMC - Fiberglass/epoxy (NEMA GR-10)

GCMC - SiC/CAS (0°)　　　　　　　　　CU - Copper

CMC - SiC/SiC (plain woven laminates)　SS - Stainless steel

TABLE VI. - COORDINATES (x-y) OF ONE EDGE OF A SPECIMEN WITH A

41.9-CM-RADIUS TRANSITION-REGION CONTOUR.

Number	x, cm	y, cm	σ_x (a)	Number	x, cm	y, cm	σ_x (a)
1	0.762	0.50800	1.00000	28	2.476	0.54311	0.93536
2	.825	.50803	.99994	29	2.540	.54574	.93084
3	.889	.50819	.99963	30	2.603	.54845	.92624
4	.952	.50842	.99918	31	2.667	.55132	.92142
5	1.016	.50877	.99849	32	2.730	.55427	.91652
6	1.079	.50919	.99766	33	2.794	.55729	.91155
7	1.143	.50974	.99659	34	2.857	.56043	.90645
8	1.206	.51036	.99538	35	2.921	.56365	.90127
9	1.270	.51109	.99395	36	2.984	.56698	.89597
10	1.333	.51191	.99237	37	3.048	.57039	.89062
11	1.397	.51280	.99064	38	3.111	.57392	.88514
12	1.460	.51381	.98870	39	3.175	.57752	.87962
13	1.524	.51493	.98654	40	3.238	.58124	.87399
14	1.587	.51613	.98425	41	3.302	.58504	.86831
15	1.651	.51741	.98181	42	3.365	.58896	.86254
16	1.714	.51881	.97917	43	3.429	.59295	.85674
17	1.778	.52032	.97633	44	3.492	.59706	.85084
18	1.841	.52191	.97336	45	3.556	.60124	.84492
19	1.905	.52357	.97026	46	3.619	.60551	.83897
20	1.968	.52539	.96689	47	3.683	.60992	.83289
21	2.032	.52725	.96348	48	3.746	.61438	.82685
22	2.095	.52923	.95988	49	3.810	.61899	.82069
23	2.159	.53129	.95617	50	3.873	.62364	.81457
24	2.222	.53346	.95228	51	3.937	.62841	.80839
25	2.28	.53570	.94829	52	4.000	.63329	.80215
26	2.34	.53807	.94412	53	4.022	.63500	.80000
27	2.413	.54055	.93979				

[a]Nominal value of σ_x along the transition region contour and normalized with respect to the nominal value of σ_x in the gage section.